


Sunlight-sensitive carbon dots for plant immunity priming and pathogen defence

Erfeng Kou¹, Zhongxu Luo¹, Jingyi Ye¹, Xu Chen¹, Dan Lu¹, Markita P. Landry², Honglu Zhang³ and Huan Zhang^{1,*} 

¹School of Agriculture and Biology, Shanghai Jiao Tong University, Shanghai, China

²Department of Chemical and Biomolecular Engineering, University of California, Berkeley, CA, USA

³School of Sensing Science and Engineering, School of Electronic Information and Electrical Engineering, Shanghai Jiao Tong University, Shanghai, China

Received 22 January 2025;

revised 24 February 2025;

accepted 27 February 2025.

*Correspondence (Tel +86 2134205177;
fax +86 2134205177; email zhang_huan@sjtu.edu.cn)

Summary

Global food production faces persistent threats from environmental challenges and pathogenic attacks, leading to significant yield losses. Conventional strategies to combat pathogens, such as fungicides and disease-resistant breeding, are limited by environmental contamination and emergence of pathogen resistance. Herein, we engineered sunlight-sensitive and biodegradable carbon dots (CDs) capable of generating reactive oxygen species (ROS), offering a novel and sustainable approach for plant protection. Our study demonstrates that CDs function as dual-purpose materials: priming plant immune responses and serving as broad-spectrum antifungal agents. Foliar application of CDs generated ROS under light, and the ROS could damage the plant cell wall and trigger cell wall-mediated immunity. Immune activation enhanced plant resistance against pathogens without compromising photosynthetic efficiency or yield. Specifically, spray treatment with CDs at 240 mg/L (2 mL per plant) reduced the incidence of grey mould in *N. benthamiana* and tomato leaves by 44% and 12%, respectively, and late blight in tomato leaves by 31%. Moreover, CDs (480 mg/L, 1 mL) combined with continuous sunlight irradiation (simulated by xenon lamp, 9.4×10^5 lux) showed a broad-spectrum antifungal activity. The inhibition ratios for mycelium growth were 66.5% for *P. capsici*, 8% for *S. sclerotiorum* and 100% for *B. cinerea*, respectively. Mechanistic studies revealed that CDs effectively inhibited mycelium growth by damaging hyphae and spore structures, thereby disrupting the propagation and vitality of pathogens. These findings suggest that CDs offer a promising, eco-friendly strategy for sustainable crop protection, with potential for practical agricultural applications that maintain crop yields and minimize environmental impact.

Keywords: carbon dots, photosensitivity, plant immunity, pathogen defence, antifungal activity.

Introduction

Extreme weather conditions and pathogenic microorganisms pose major threats to global food production. Plant pathogens such as *Sclerotinia sclerotiorum* (*S. sclerotiorum*), *Botrytis cinerea* (*B. cinerea*) and *Phytophthora capsici* (*P. capsici*) are highly destructive, causing sclerotinia stem rot, grey mould and late blight, which lead to significant economic losses worldwide (Cheung *et al.*, 2020; Lamour *et al.*, 2011; Lin *et al.*, 2024). These pathogens have a broad host range, affecting many key agricultural crops and resulting in annual economic losses exceeding one billion US dollars (Lamour *et al.*, 2011). Current strategies to combat plant pathogen infections include the use of fungicides and breeding of disease-resistant varieties (El-Baky and Amara, 2021). However, the overuse of fungicides can lead to pathogen resistance and environmental pollution (El-Baky and Amara, 2021), while traditional breeding is time-consuming, costly and difficult to produce varieties with durable resistance or broad-spectrum pathogen resistance, as pathogens evolve to evade recognition (Nelson *et al.*, 2018).

Plants have evolved sophisticated immune systems to defend against pathogens, including mechanisms like pattern-triggered immunity (PTI) and effector-triggered immunity (ETI) (Hou

et al., 2021). Cell-surface pattern recognition receptors (PRRs) detect microbe-associated molecular patterns (MAMPs) or damage-associated molecular patterns (DAMPs), triggering PTI and a cascade of immune signalling events. In response, pathogens produce virulence factors (effectors) that suppress PTI and trigger ETI (Ge *et al.*, 2022; Yoshioka *et al.*, 2023). Inspired by these natural immune responses, researchers have identified various elicitors, such as proteins, oligosaccharides, peptides, lipids, small molecule metabolites and compounds mimicking DAMPs/PAMPs that can enhance plant immunity and protect against pathogens (Agrawal *et al.*, 2002; Chen *et al.*, 2024; Dewen *et al.*, 2017). For example, flg22, a 22-amino acid peptide derived from pathogenic bacteria, is a well-known bio-inducer that activates plant defence response and enhance disease resistance (Bethke *et al.*, 2009; Jelenska *et al.*, 2017). Despite their potential, bio-elicitors face challenges such as complicated synthesis methods, high production costs and potential negative effects on plant growth and crop yields (Yang *et al.*, 2022).

Recent advances in nanomaterials such as silver, copper, silicon, selenium and carbon have been reported to help plants defend against pathogens and improve disease resistance (El-Shetehy *et al.*, 2021; Guo *et al.*, 2023; Jo *et al.*, 2009;

Please cite this article as: Kou, E., Luo, Z., Ye, J., Chen, X., Lu, D., Landry, M.P., Zhang, H. and Zhang, H. (2025) Sunlight-sensitive carbon dots for plant immunity priming and pathogen defence. *Plant Biotechnol. J.*, <https://doi.org/10.1111/pbi.70050>.

Karimi, 2019; Khosropour et al., 2023; Shang et al., 2023; Xia et al., 2021). Carbon dots (CDs), zero-dimensional carbon-based nanomaterials, offer low cost, small size, high biocompatibility and versatile modification capabilities (Liu et al., 2020). They have shown promising applications in plants. For instance, CDs can improve plant production by enhancing photosynthetic processes, including electron transport (Chandra et al., 2014; Huang et al., 2023), CO₂ assimilation and fixation (Li et al., 2019; Sukhanova, 2010), light conversion and capture (Li et al., 2021; Wang et al., 2021; Wei et al., 2017) and nutrient uptake (Jing et al., 2022; Kou et al., 2021). Moreover, CDs have been reported to act as light converters and enhance photosynthesis, thereby promoting the growth and development of plants (Guirguis et al., 2023; Hu et al., 2024). CDs also improve plant tolerance to biotic and abiotic stresses by scavenging reactive oxygen species (ROS), enhancing antioxidant enzyme activity and acting as electron acceptors (Li et al., 2022; Liu et al., 2020, 2024; Wang et al., 2022; Yang et al., 2022). Furthermore, functionalized CDs have been explored for chemical and gene delivery into plants (Jeon et al., 2023; Santana et al., 2022; Sharma et al., 2024). CDs' excellent photoelectric properties enable them to regulate ROS, which are utilized for bacterial inhibition and tumour therapy in animals (Cheng et al., 2024; Wang et al., 2017; Zhang et al., 2023). However, their potential for ROS regulation to protect plants has not been fully explored.

In this study, we developed sunlight-sensitive, degradable CDs that generate ROS and investigated their ability to prime plant immunity and exhibit antifungal effects. Our results demonstrate that CDs at lower concentration (240 mg/L, 2 mL per plant) can enhance pathogen resistance of *Nicotiana benthamiana* (*N. benthamiana*) and tomato (*Solanum lycopersicum*, L) plants under natural growth conditions by inducing cell wall-mediated immunity, triggering a cascade of immune responses, such as ROS bursts, MAPK cascades, the accumulation of phytoalexins and defence phytohormones. At higher concentrations (>480 mg/L) and with continuous light irradiation, CDs deactivated *P. capsici*, *B. cinerea* and *S. sclerotiorum* pathogens by damaging the structures of their hyphae and spores, thereby reducing their infection ability. In short, compared to bio-elicitors, like flg 22, CDs have a simple and cost-effective synthesis process. Notably, CDs not only effectively induce plant immune responses but also demonstrate significant potential for enhancing plant defence towards fungal diseases without compromising their growth. These findings suggest that sunlight-sensitive CDs offer a novel and sustainable strategy for crop protection, broadening their application in plant disease management.

Results and discussions

Preparation and characterization of CDs

CDs were synthesized using o-phenylenediamine and L-cystine by a one-step hydrothermal method in aqueous solution according to our previous report (Figure 1a) (Kou et al., 2023). The synthesized CDs were positively charged, with a zeta potential of +16.4 mV (Figure S1) and showed an emission peak at 485 nm upon excitation at 424 nm (Figure 1b). Transmission electron microscope (TEM) imaging (Figure 1c) and atomic force microscopy (AFM) (Figure 1d) indicated that the CDs size distribution was in 2–5 nm with a 0.26 nm lattice spacing, corresponding to diffraction facets of graphite-like (020) core structures (Nie et al., 2014; Zhang et al., 2022). The functional groups of the CDs were characterized with Fourier transform infrared (FTIR)

spectroscopy. As shown in Figure 1e, a wide stretching peak at 3480 cm⁻¹ was ascribed to the stretching of primary –NH₂ and –OH groups. The bands at 2920, 1650, 1510 and 1321 cm⁻¹ correspond to stretching vibrations of C–C, C=O/C=N, C=C and CO–NH, respectively (Ru et al., 2023; Zhang et al., 2022). The vibrational bands from 1201 to 880 cm⁻¹ correspond to the vibrations of C–C/C–N/C–OH⁴⁶. Peaks at 2560 and 1184 cm⁻¹ can be attributed to the stretching of S–H and C–S (Hu et al., 2017). The above results suggested that CDs contain various electron-enriched function groups, such as –NH₂, –COOH and –OH, providing these CDs with photo-electron transfer properties with photocatalytic activity.

The ultraviolet–visible (UV–vis) absorption spectra showed maximal absorption peaks at 228 and 274 nm (grey line, Figure 1f), corresponding to aromatic π–π* transitions of C=C and C=N in the core and the n–π* transition of C=O and C–O on the surface of CDs (Lu et al., 2017; Ru et al., 2021). Upon irradiation by a handheld UV light (1950 lux) with 365 nm wavelength emission, a distinct peak at ~452 nm emerged and gradually enhanced with the prolongation of irradiation time, whereas the absorption peak at 228 nm of C=C decreased with the time (Figure 1f). Based on the abundant electron-rich groups and cystine residues of CDs, we speculate this newly emerging peak might relate to the oxidation of sulphur- and nitrogen-containing surface groups of CDs. At the same time, FTIR and UV–vis characteristic peaks of CDs gradually disappeared after 90-days under natural sunlight condition (Figure S2), indicating the degradability and environmental compatibility of CDs. The electron spin resonance (ESR) spectra demonstrated that CDs could generate reactive oxygen species (ROS) under the irradiation of sunlight (simulated by xenon lamp, 5000 W/m²), including singlet oxygen (¹O₂), superoxide radicals (O₂⁻) and hydroxyl radicals ([•]OH) (Figure 1g). Therefore, we believe that surface defects and functional groups of the CDs (such as –OH) were involved in the generation of ROS radicals under light irradiation. Then the radicals can attack the CDs in multiple ways, such as abstracting H-atom, attacking the C=C bonds via hydroxylating, and thus resulting in the degradation of CDs, consistent with previous study (Liu et al., 2021; Wu et al., 2013; Yu et al., 2016; Yue et al., 2019).

CDs trigger a plant immune response against pathogen infection

ROS, including ¹O₂, O₂⁻, [•]OH and H₂O₂ play dual roles in plant biology. Elevated levels of ROS may disrupt the cellular redox balance and lead to oxidative damage, whereas low levels of ROS can act as crucial signalling molecules in plants (Mittler, 2017). Since the CDs prepared in this study can generate ROS (including ¹O₂, O₂⁻, [•]OH) under light irradiation. We conjectured that the ROS generated by CDs could trigger the plant defence responses. To confirm this speculation, we first characterized the location of CDs after 4 h spray treatment. As the results shown in Figure S3, the CDs were observed both on the surface and inside the leaf. Given that CDs can generate ROS in situ under light exposure, the ROS could damage the cuticle and cell wall and act as crucial signalling molecules to trigger plant immune responses, such as ROS burst and lignin deposition as reported (Bacete et al., 2017; Denness et al., 2011). Then, we examined whether CDs could induce ROS bursts in plants. Flg22 has been proved to trigger the local and systemic immune responses in plants along with the rapid ROS burst (Jelenska et al., 2017; Yuan et al., 2021). Herein, flg22 was employed as a positive control group. The

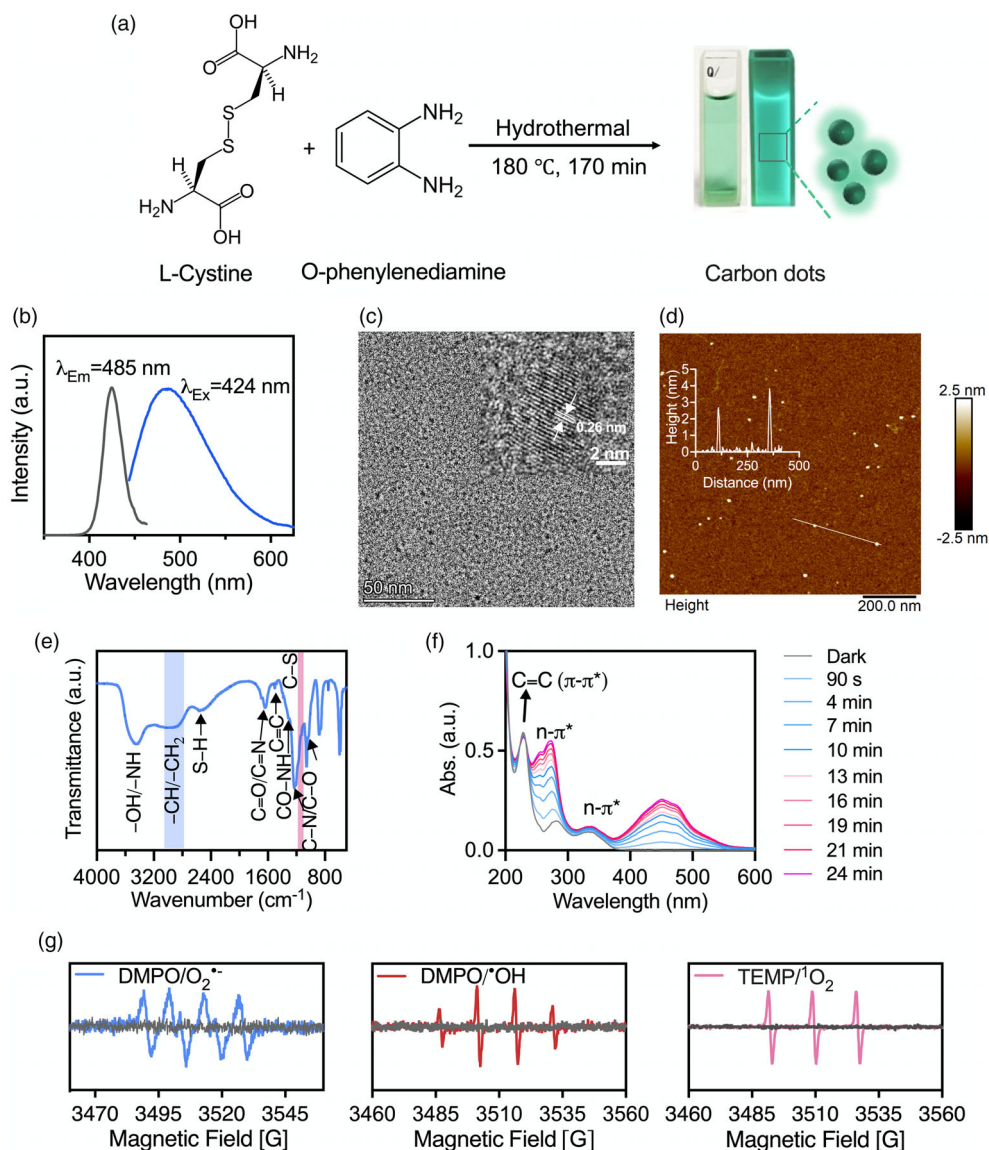


Figure 1 Preparation and characterization of CDs. (a) Scheme of CDs synthesis. (b) Fluorescence spectra of CDs. (c) TEM image of CDs and the inset high-resolution TEM image shows a lattice spacing of 0.26 nm. Scale bar = 50 nm or 2 nm. (d) AFM image of the CDs. Inset: Height profile of CDs along with the white line. Scale bar = 100 nm. (e) FTIR spectrum of CDs. (f) UV-vis absorption spectra of CDs before and after 365 nm wavelength irradiation by handle UV light for various times. (g) ESR spectra of ROS generated by CDs after irradiation with sunlight (simulated by xenon lamp, 5000 W/m²) for 10 min, showing the generation of O₂^{•-} (blue line), [•]OH (red line) and ¹O₂ (pink line). Dark grey line is the spectra of CDs under the dark condition.

leaves of one-month-old *N. benthamiana* were sprayed with 2 mL aqueous solutions containing 240 mg/L CDs or 250 µg/L flg22, then ROS bursts at various time points were monitored using 2, 7-dichlorofluorescein diacetate (H₂DCF-DA) fluorescence dye staining method (Yuan *et al.*, 2021). As shown in Figure 2a and Figure S4, flg22- and CDs-treated leaves showed an obvious green fluorescence signal after treatment for 6 h. Also, CDs at 240 mg/L concentration triggered the ROS burst at 4 h and then lasted and weakened after 8 h (Figure 2a). We also observed the ROS burst in tomato leaves 6 h after foliar spray treatment with same concentration of CDs (Figure S5). ROS signal in plant apoplast is considered as vital secondary messengers that mediate downstream immune responses in PTI and ETI (Nosaka and Nosaka, 2017; Wu *et al.*, 2023; Yoshioka *et al.*, 2008). Herein,

the ROS burst indicates that CDs could induce immune response in plant (Qi *et al.*, 2017; Wu *et al.*, 2023).

Plants have evolved sophisticated defence systems, such as superoxide dismutase (SOD), peroxidase (POD) and catalase (CAT) to eliminate excessive ROS and maintain redox homeostasis (Apel and Hirt, 2004; Mittler *et al.*, 2004). To further validate the in planta ROS burst induced by CDs treatment, the enzymatic activity of SOD, POD and CAT in tomato leaves were evaluated 24 h after foliar treatment with various concentration of CDs. As shown in Figure 2b, the enzyme activity of SOD significantly enhanced after treatment of 160 and 240 mg/L CDs and the enzyme activity of POD was significantly improved after treatment of 240 mg/L CDs. These improved activity of SOD and POD implied that CDs spray treatment disturbed the redox

4 Erfeng Kou et al.

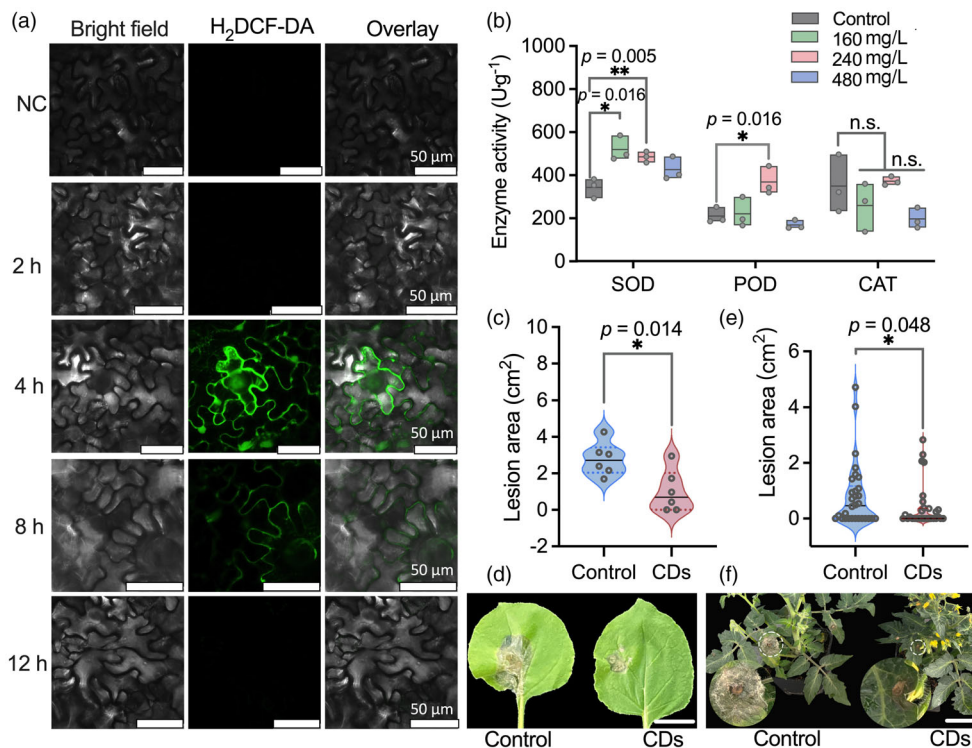


Figure 2 CDs induce ROS bursts and enhance pathogen defence of *N. benthamiana* and tomato. (a) Characterization of ROS burst in *N. benthamiana* leaves sprayed with deionized water (negative control, NC) or CDs aqueous solution (240 mg/L). Scale bars = 50 μm . (b) Enzyme activity of SOD, POD and CAT in tomato leaves after 24 h sprayed with CDs at final concentrations of 160, 240 and 480 mg/L, respectively. Error bar means \pm s.e.m.; $n = 3$. P -values resulted from one-way ANOVA multiple-comparison tests. $*P < 0.05$, $**P < 0.01$. n.s., not significant. Lesion areas (c) and representative image (d) of *N. benthamiana* leaves after inoculated with *B. cinerea* mycelium for 5 days. Scale bar = 3 cm. Lesion areas (e) and image of tomato leaves (f) after inoculated with *B. cinerea* mycelium for 5 days. Scale bar = 3 cm. Individual data of points in (c) and (e) scattered around the mean \pm s.e.m.; Data points in (c), $n = 6$. Data point in (e), $n = 30$ (control) or 29 (CDs). P -values resulted from t tests between control and treatment. $*P < 0.05$.

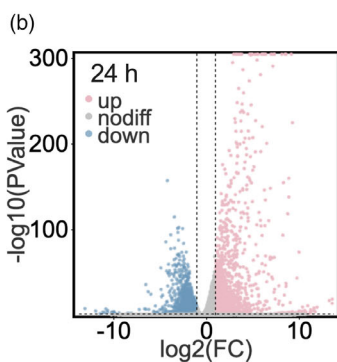
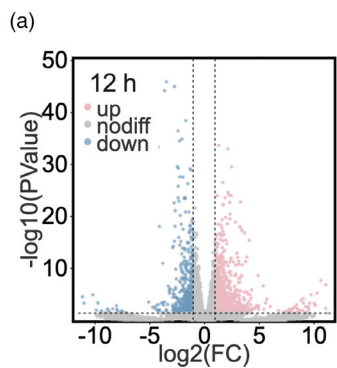
homeostasis, which are complementary to the results of ROS bursts and in alignment with the performance of previously reported elicitors (Görlach et al., 1996; Yang et al., 2022; Zhu et al., 2024).

To further confirm the immune priming ability of CDs, we sprayed *N. benthamiana* or tomato leaves with 240 mg/L CDs solution (2 mL per plant). The control leaves were sprayed with the same volume of deionized water. Then these pre-treated leaves were infected with a piece of agar (0.6 cm in diameter) containing *B. cinerea* mycelium or 20 μL *P. capsici* spores (1×10^5 zoospores per mL). Subsequently, these infected plants were returned to the plant incubator and cultivated under standard conditions. The incidence ratio was calculated after 5 days, and the incidence of grey mould of *N. benthamiana* and tomato leaves were reduced by 33% and 12%, respectively (Figure S6a, b). The lesion areas in *N. benthamiana* leaves (Figure 2c, d) and tomato leaves (Figure 2e, f) were also significantly decreased by in CDs-sprayed leaves, compared to the control groups. Moreover, the incidence of late blight of CDs-sprayed tomato leaves

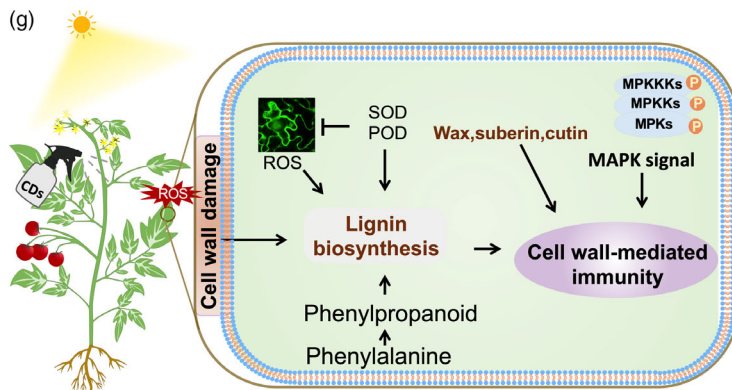
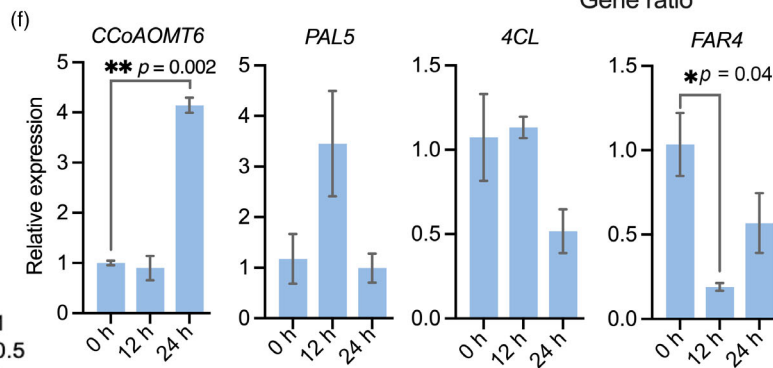
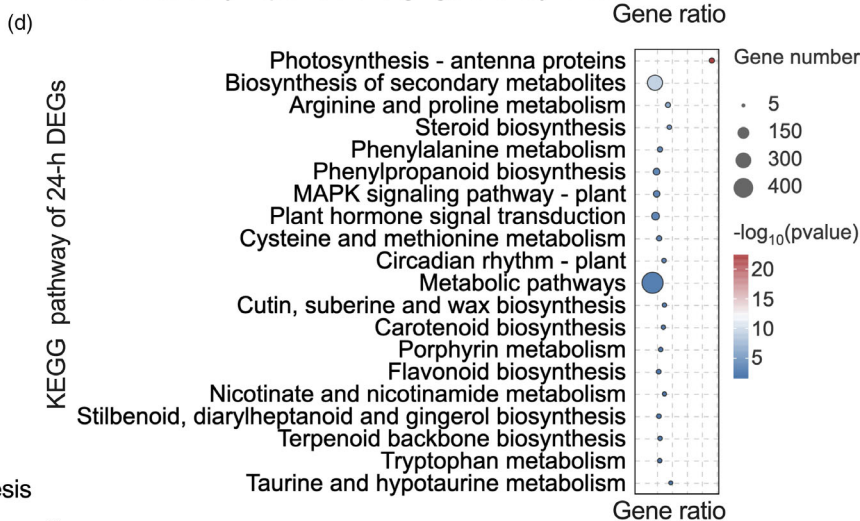
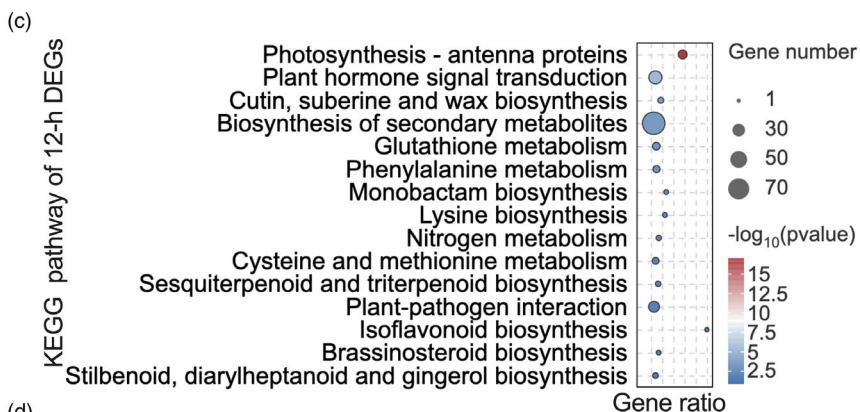
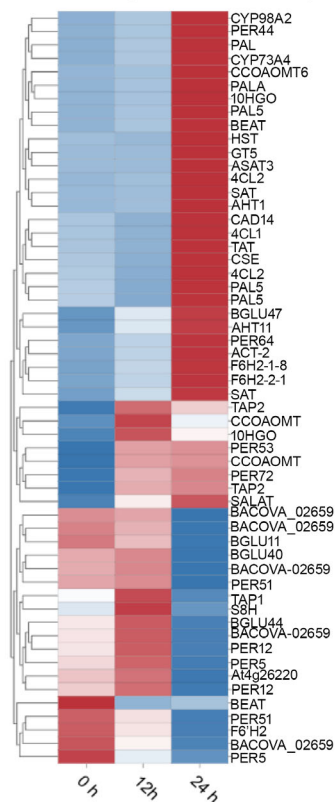
decreased by 31% (Figure S7) after infection with 20 μL *P. capsici* spores for 7 days. These results confirmed that pretreatment of CDs spray can induce ROS bursts and trigger the plant defence response, which sequentially enhanced plant disease resistance to pathogens, like *P. capsici* and *B. cinerea*.

To explore the mechanism of defence response of plants induced by CDs, we performed a transcriptomic analysis of tomato leaves at 12 and 24 h after spray treatment with 240 mg/L CDs. As shown in Figure S8a, three independent technical replicates of our transcriptomic analysis were well clustered, indicating that our transcriptomic analysis is reproducible. In addition, we verified the expression levels of 12 DEGs from the first 10 KEGG pathway using qRT-PCR, and the results were consistent with those of RNA-seq (Figure S9), further proving that the transcriptome results were reliable. The number of differential ($P < 0.05$) expression genes (DEGs) induced by CDs pretreatment after 12 h is 1, 034, and this number increased to 4, 011 at 24 h timepoint (Figure 3a, b, Figure S8b, c). Gene ontology (GO) annotation indicated that the DEGs following 12 h of CDs

Figure 3 CDs spray (240 mg/L) induced the responses to stimulus and stress acclimation in tomato. Volcano diagram of DEGs after CDs treatment for 12 h (a) and 24 h (b). KEGG enrichment pathways ($P < 0.05$) of DEGs after CDs treatment for 12 h (c) and 24 h (d). (e) The DEGs in lignin and suberin biosynthesis pathways after CDs treatment for 12 and 24 h. (f) The relative expression level of *CCoAOMT6*, *PAL5*, *4CL* and *FAR4* measured by qRT-PCR. Data show mean \pm s.e.m. The error bars in the columns represent the s.e.m.; $n = 3$. P -values resulted from t tests between 0 and 12 h or 24 h. $*P < 0.05$, $**P < 0.01$. (g) Schematic of immune pathways triggered by CDs spray in tomato.



(e) DEGs of henylpropanoid biosynthesis



treatment were significantly ($P < 0.05$) enriched in response to stress, stimulus and cell endogenous stimulus as well as oxidation and defence (Figure S8d), suggesting CDs pretreatment induced defence response in plant leaves. GO annotation of DEGs at 24 h CDs treatment demonstrate that these DEGs are significantly enriched in biological processes, such as sulphur compound metabolic processes, oxidoreductase activity, anion transmembrane transporter activity, as well as response to abiotic and endogenous stimuli (Figure S8e). These results indicate that CDs can act as external stimulant to activate the defence response of plant leaves.

To further elucidate the function of CDs, we systematically analysed the function of DEGs via the KEGG (Kyoto encyclopaedia of genes and genomes) database, aiming to link genomic information with higher order functional information. As shown in Figure 3c, DEGs of 12 h CDs treatment (240 mg/L) groups are significantly enriched in metabolic process of cysteine and methionine, biosynthesis of flavonoids, sterols and glutathione, as well as phytohormones signal pathways. DEGs of 24 h CDs treatment (240 mg/L) was significantly enriched in photosynthesis-antenna proteins, signal transduction of phytohormones and mitogen-activated protein kinase (MAPK) cascades, biosynthesis of steroids, phenylalanine, phenylpropanoids, cutin and wax, as well as various amino acid metabolic pathways (Figure 3d). Calcium ion (Ca^{2+}) influx, ROS burst, MAPK cascades and the response of defence hormones are considered as the first line of plant's protective reaction, whereby these primary signals can subsequently mediate the transcriptional regulation of cell wall reinforcement and phytoalexins biosynthesis (Nürnberg and Scheel, 2001; Zhang and Zhang, 2022). Cutin, wax and lignin can act as primary defensive barriers in plants, which protect the plant cell wall from hydrolysis by pathogenic bacteria, thereby enhancing their disease resistance (Molina et al., 2024; Raffaele et al., 2009; Singh and Chandrawat, 2017; Swaminathan et al., 2022; Williams et al., 2002).

We noticed that genes in the phenylpropane biosynthesis pathway were significantly regulated by the CDs treatment (Figure 3e). It is well known that one of main metabolites of phenylpropanoid pathways is lignin, which acts as one of main components of cell wall during the process of thickening the secondary wall (Vanholme et al., 2010). When cell wall damage occurs, compensatory mechanisms, such as the biosynthesis of lignin and suberin, are activated (Bacete et al., 2017; Denness et al., 2011; Wang and Balint-Kurti, 2016). Given the oxidation property of ROS, we suspect that ROS generated by CDs led to cell wall damage in tomato leaves, finally initiating the synthesis of lignin and suberin. Interestingly, we found that the genes, encoding key enzymes in lignin biosynthesis, such as phenylalanine ammonia-lyase (PAL), 4-coumarate-CoA ligase (4CL), cinnamyl alcohol dehydrogenase (CAD) and caffeoyl CoA o-methyltransferase (CCoAOMT), were significantly up-regulated by CDs treatment (Figure 3e). We further confirmed the expression level of these genes after CDs treatment for 12 and 24 h by qRT-PCR. As shown in Figure 3f, consisting with results of RNA-seq, the relative expression of CCoAOMT6 in tomato leaves was significantly up-regulated by CDs treatment after 24 h. PAL5 was slightly enhanced by CDs treatment at 12 h. CDs treatment do not effect on the 4CL expression. Suberin also is located on the cell walls, contributing to cell wall structural integrity and protective functions (Domergue et al., 2010). FAR4, one of the key genes encoding fatty acyl-coenzyme A reductases, is associated with suberin deposition (Domergue et al., 2010). In

this study, we found CDs treatment markedly down-regulated the expression of FAR4 at 12 h (Figure 3f). Previous research has proved that the POD enzyme mediated lignin biosynthesis with the participation of ROS (Denness et al., 2011). Therefore, the improved POD and SOD activity and the generation of ROS under the CDs treatment might be related to lignin biosynthesis. Plants have dedicated mechanism to maintain cell wall integrity which comprises a diverse set of plasma membrane-resident sensors and pattern recognition receptors (Bacete et al., 2017). Our results demonstrate that CDs enhance plant defence ability through cell wall-mediated disease resistance. Specifically, the CDs generated ROS on the leaf surface and damage the cell wall, which activated the cell wall-mediated immune responses, including the deposition of lignin, suberin, wax and cutin, as well as ROS burst, ultimately improving the defence ability of plants (Seifert and Blaukopf, 2010).

Given that continuous exposure to high concentration, ROS would lead to oxidative toxic and thus impact plant growth and development (Apel and Hirt, 2004). Herein, we evaluated the impact of CDs treatment on plant growth. Photosystem II (PSII) activity is a common metric for plant growth evaluation to abiotic and biotic stress (Murchie and Lawson, 2013). Our results indicated that, compared to deionized water sprayed group, *N. benthamiana* leaves sprayed with CDs solutions with various concentrations (240, 480, 960 and 2400 mg/L) after 72 h showed no differences in quantum yield of PSI (YI) (Figure S10a) and PSII (YII) (Figure S10b), as well as maximum quantum efficiency of PSII photochemistry (Fv/Fm) (Figure S10c). Moreover, compared to the control groups (sprayed with deionized water), CDs-sprayed (with various concentrations, from 240 to 2400 mg/L) *N. benthamiana* plants exhibited no significant differences in the fresh weight and dry weight of the aboveground yields after a period of 7 days (Figures S10d and S11a,b). More importantly, CDs (240 and 480 mg/L) sprayed tomato showed no differences in fruit yields after treatment for 30 days (Figure S12). The above results manifested that CDs treatments exhibited minimal interference in plant growth and yields, which further demonstrates the potential of CDs as a promising immune priming tool to enhance the plant resistance to the pathogens.

Sunlight-induced broad-spectrum antifungal ability of CDs

Since the CDs we synthesized are sunlight-sensitive and could generate moderate quantities of ROS at high concentrations, we investigated the antifungal ability of CDs under constant sunlight irradiation (simulated by a xenon lamp, 9.4×10^4 lux), which would be ideal for practical field applications for crops. We first estimated the inhibition efficiency of CDs at various concentrations towards *B. cinerea* mycelial growth after 30 min irradiation. As shown in Figure S13a,b, the inhibitory efficiency of CDs on mycelial growth was dose-dependent, and further quantitative analysis indicated that both 480 and 960 mg/L of CDs showed significant inhibition on hyphal growth. Then 480 mg/L CDs was chosen and *P. capsici*, *B. cinerea* and *S. sclerotiorum* were employed as oomycete and fungal models for further study of the potential antifungal ability of CDs. As shown in Figure 4a,b, compared with light treatment (Light control), dark treatment (Dark control) and CDs under dark condition (Dark + CDs), the hyphal growth of *P. capsici*, *S. sclerotiorum* and *B. cinerea* was significantly inhibited in the group of CDs with light irradiation (Light + CDs) treatment. The inhibition percentages of Light +

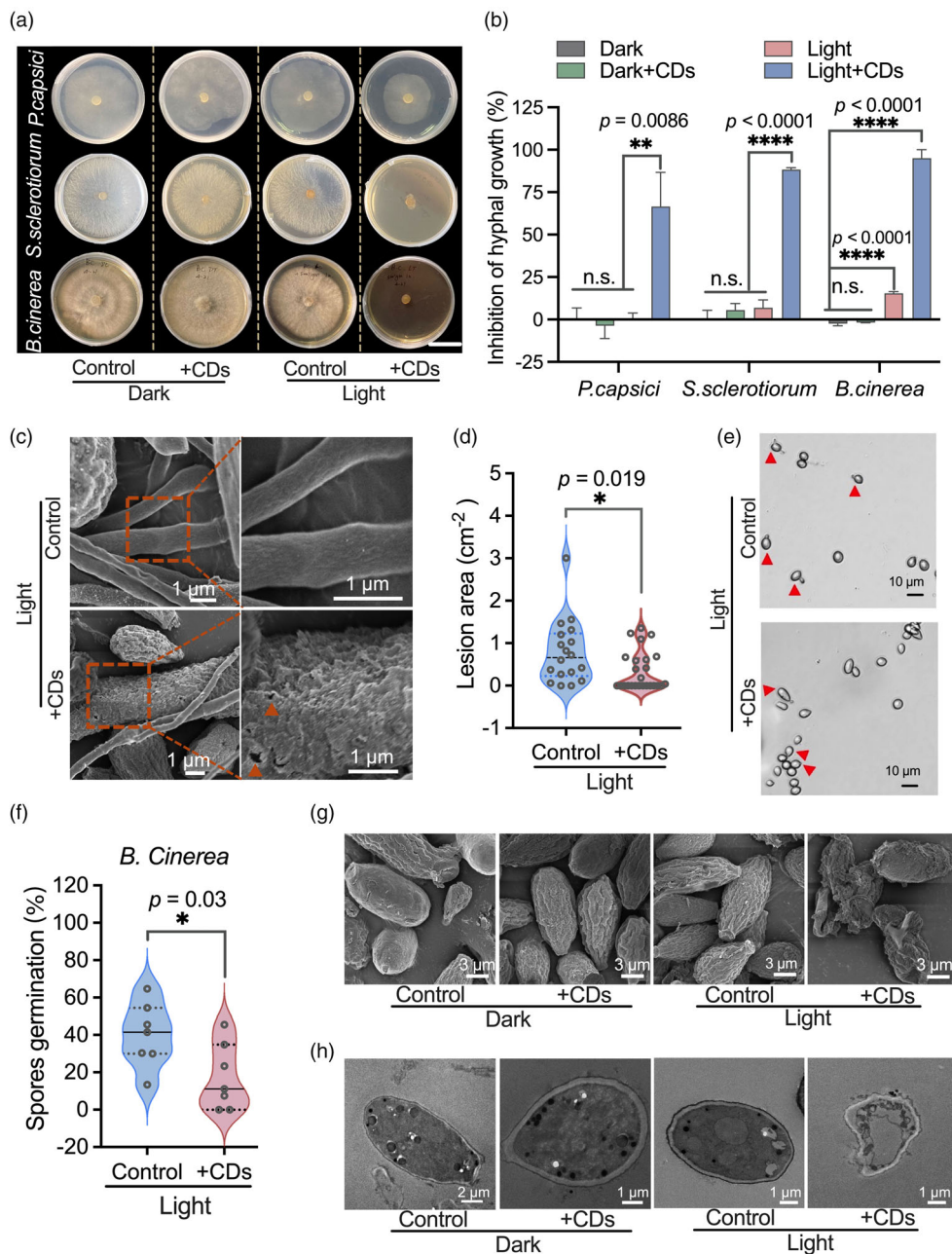


Figure 4 *In vitro* antifungal activity of CDs. (a) The images of mycelium growth on medium plates for *P. capsici*, *B. cinerea* and *S. sclerotium* under different treatment. Scale bar = 3 cm. (b) Quantitative statistical data of (a). Data show mean \pm s.e.m.; $n = 3$. P values resulted from one-way ANOVA multiple-comparison tests. $**P < 0.01$, $****P < 0.0001$, n.s., not significant. (c) SEM images of *B. cinerea* hyphae for different treatment. (d) Lesion areas of tomato leaves after infected with *B. cinerea* mycelium pre-treated by Light + CDs (480 mg/L, 1 mL) or only Light (control) for 5 days. Data show mean \pm s.e.m.; $n = 18$ (Light control) and $n = 26$ (Light + CDs). P -values resulted from unpaired t -test. $*P < 0.05$. (e) Images of *B. cinerea* spores germination after treatment of Light + CDs (480 mg/L, 1 mL) or Light (control) for 24 h. (f) Quantitative statistical data of (e). Data show mean \pm s.e.m., $n = 6$. P -values resulted from unpaired t -test. $*P < 0.05$. SEM (g) images and TEM (h) images of *B. cinerea* spores under different treatments.

CDs treatment on hyphae of *P. capsici*, *S. sclerotium* and *B. cinerea* were 66.5%, 88.3% and 100%, respectively (Figure 5b). Neither Light control nor Dark + CDs treatment showed obvious inhibition, indicating the specifically light-induced antifungal ability of the CDs. Moreover, the effective inhibitory effects on *P. capsici*, *S. sclerotium* and *B. cinerea* suggest the broad-spectrum antifungal ability of CDs.

Next, we examined the morphological structure of *B. cinerea* hyphae after 45 min irradiation under the condition of Light + CDs (480 mg/L) or Light control, since ROS can induce oxidative damage, which might lead destruction of the fungal cell wall (Apel and Hirt, 2004). As shown in Figure 4c, the scanning electron microscope (SEM) images of *B. cinerea* hyphae under Light + CDs treatment showed an obviously shrivelled surface

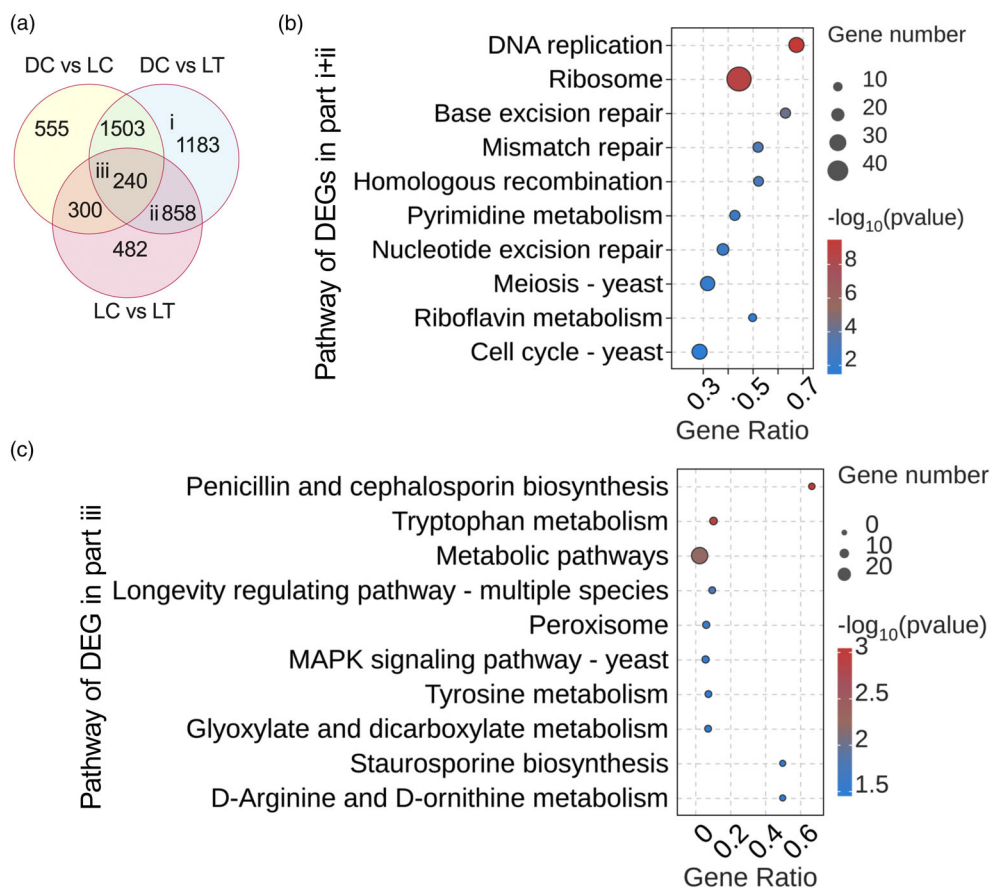


Figure 5 RNA-seq data of *B. cinerea* in different treatment. (a) Venn diagram of DEGs. DC, Dark control; LC, Light control; LT, Light + CDs. The first 10 KEGG enrichment pathway of DEGs of part i and part ii (b), and part iii (c) of (a).

with several small holes, as illustrated in the enlarged image (right, indicated by orange arrows). In contrast, the hyphae of the Light control group showed a smooth surface, indicating that ROS generated from irradiated CDs can destroy the structure of *B. cinerea* hyphae, which in return might influence its infection capacity and proliferation. To verify the above speculation, we evaluated the infection ability of *B. cinerea* hyphae after Light + CDs treatment. As shown Figure S14, the incidence ratio of tomato leaves in the control group (infected by light treated mycelium) and the treatment group (infected by 1 mL, 480 mg/L CDs + Light treated mycelium) were 89% and 46%, and the average lesion areas of leaves infected by pre-treated *B. cinerea* mycelium were 0.79 and 0.34 cm² (Figure 4d), respectively, indicating that CDs with light irradiation could effectively inhibit the infection ability of *B. cinerea*.

In a natural environment, the major transmission means of grey mould is through airborne spreading of mature conidiophores (Romanazzi and Feliziani, 2014). Once the spores fall on the plant, they can germinate and infect the plant. Hence, we evaluated the impact of CDs treatment (480 mg/L) on the germination of spores. As shown in Figure 4e,f, the percentage of germinating spores after light treatment and Light + CDs treatment for 20 min was 40.0% and 17.4%. When the light irradiation time prolonged to 30 min, the inhibition ratio of Light + CDs group reached 100% (Figure S13c). We further investigated the influence of CDs treatment on spore morphology under dark

and light conditions via SEM and TEM. The SEM and TEM images (Figure 4g,h) showed that the structure of the spores shrivelled after treatment of Light + CDs for 30 min, whereas Dark, Dark + CDs and Light only treatment barely affected the spores. All the above results indicated that the *in situ* generated ROS from CDs damaged the structure of hyphae and spores, directly inhibiting the proliferation and growth of pathogens and thus reduced their infection capacity.

Antifungal mechanism of CDs towards *B. Cinerea*

To further investigate the antifungal mechanism of CDs, we explored the effect of CDs + Light treatment (480 mg/L, 1 mL) to *B. cinerea* at the transcriptome level by RNA-Seq. Principal component analysis (PCA) results in Figure S15a indicated that our three independent replicates have a high correlation, indicating the reliability of our data. Based on the above results, we analysed DEGs induced by different treatments with a Venn diagram (Figure 5a). Light treatment (Light control, LC) was set to avoid any interference of light irradiation. The 2041 DEGs of part i and ii are induced by the light + CDs treatment. Two hundred and forty genes in part iii were identified as DEGs specifically induced by CDs treatment compared with Dark control (DC) and LC. As shown in Figure S15b, the 10 highly enriched GO terms of the 2041 DEGs induced by the CDs treatment were largely associated with DNA replication and structural constituent of ribosome. The KEGG enrichment results demonstrated that the

2041 DEGs were significantly enriched in genetic information processing (base excision repair, translation), cellular processes (cell growth and death) and vitamin metabolism (Figure 5b). Organisms can utilize base excision to repair or eliminate broken/nicked/oxidized DNA, damaged bases and proteins, induced by endogenous or external genotoxicants, such as ROS, to maintain genomic integrity (Hegde *et al.*, 2008; Mittler, 2017). Therefore, our results demonstrated that $^1\text{O}_2$, O_2^- and $^{\cdot}\text{OH}$ produced by CDs under light irradiation damaged DNA of *B. cinerea*. The GO terms of 240 DEGs specifically induced by CDs demonstrated that CDs disturbed the redox homeostasis of *B. cinerea* (Figure S15c). The KEGG enrichment results indicated that these 240 DEGs were significantly enriched in tryptophan and tyrosine metabolism pathway and peroxisome, penicillin and cephalosporin biosynthesis process (Figure 5c). Peroxisomes were reported to function in redox signalling whereas glutathione can directly alleviate oxidative damage (Chen *et al.*, 2016; Williams *et al.*, 2002). Penicillin and cephalosporin are well-known antibiotics (de Weck, 1983). Thus, combining with the results of structure and morphology of *B. cinerea* spores and hyphae after Light + CDs treatment, we speculate that ROS produced by CDs under constant irradiation not only caused oxidative damage to membrane structure of pathogens, but also damage their DNA, resulting in deactivation of spores and hyphae.

Conclusion

In this study, we developed sunlight-sensitive, biodegradable CDs capable of generating ROS. Our results demonstrate that CDs could play a dual role in plant protection: acting as an elicitor to prime plant immunity and as a biocompatible fungicide with broad-spectrum antifungal activity. At a low concentration (240 mg/L, 2 mL per plant) via leaf spraying, CDs generate moderate ROS under natural growth conditions, which can induce cell wall damage-mediated immunity and trigger a cascade of immune responses, such as ROS bursts, MAPK cascades, the accumulation of phytoalexins and defence phytohormones. This immune priming effect significantly enhanced the plant's immune response and improved resistance to pathogen infections after 24 h of pretreatment. At higher concentrations (≥ 480 mg/L, 1 mL) with continuous light irradiation, CDs generated ROS *in situ*, causing oxidative damage to structures of *P. capsici*, *S. sclerotiorum* and *B. cinerea*. This oxidative stress rendered pathogenic mycelia and spores inactive, effectively preventing plant disease occurrence and spread. The dual functionality of CDs as both a plant immune priming agent and fungicide represents a promising advancement in sustainable crop protection strategies. Moreover, the biodegradable nature and low toxicity of CDs make them a unique and safe alternative to chemical pesticides and fungicides, promoting a more environmentally friendly approach to crop protection. These properties position CDs as a viable solution for translating from laboratory research to practical field applications, offering a safe and effective way to enhance crop resilience and productivity in agriculture.

Materials and methods

Preparation of CDs

CDs were prepared as previously described (Kou *et al.*, 2023). However, since the materials synthesized earlier had larger

sizes, which were not conducive to degradation, we adjusted the concentration of the synthesis precursors and the duration of the hydrothermal reaction. CDs were synthesized through a hydrothermal method using O-phenylenediamine (Macklin, Shanghai, China), L-cystine (Macklin) and 98% sulphuric acid (Sinopharm, Shanghai, China) as previously reported. In brief. To elaborate, 0.3 g O-phenylenediamine and 0.1 g L-cystine were dissolved in 30 mL of deionized water. Subsequently, 3 mL of sulphuric acid was added and the mixed solution. The above mixture solution was transferred to a polytetrafluoroethylene reactor and heated at 180 °C for 170 min to get the CDs. The prepared CDs aqueous solution was purified in water with a cellulose dialysis bag (100–500 Da, Yuanye, Shanghai, China) for 12 h to remove unreacted precursors. The water was changed every 4 h. The prepared CDs was lyophilized to confirm the concentration. The above prepared CDs aqueous solution was further diluted to specific concentration using deionized water.

CDs characterization

The fluorescence spectra of CDs (480 mg/L) were measured at room temperature by FLS1000 (Edinburgh Instruments, Livingston, West Lothian, UK). For AFM imaging for CDs, 10 μL of 240 mg/L CDs was dropped onto mica surface for 5 min. And 20 μL of 1xTM buffer was dropped onto the mica surface. The CDs imaging was performed in liquid phase mode using Bruker multimode 8 (Bruker Corporation, Billerica, MA, USA). TEM imaging was performed with Talos L120C 36 G2 transmission electron microscope operating at an accelerating voltage of 120 kV. The UV-vis spectra of the CDs (480 mg/L) were obtained with UV-2600i (Shimadzu corporation, Kyoto, Japan) with or without 365 nm wavelength irradiation through a handheld light (1950 lux). The Zeta potential of CDs was measured in Zetasizer ultra (Malvern Panalytical, Malvern, UK) with 240 mg/L concentration. Fourier transform infrared (FTIR) spectra were recorded by Nicolet 6700 instrument (Thermo Fisher Scientific, Waltham, MA, USA). Reactive oxygen species measurements were carried out on an electron paramagnetic resonance spectrometer (Bruker 300, Bruker Corporation, Billerica, MA, USA) using 240 mg/L-CDs. For Zeta potential, FTIR and ROS measurements, the concentration of CDs was 480 mg/L. The spin-trapping agent employed for the sequestration of hydroxyl radicals and superoxide anion radicals was 5, 5-dimethyl-1-pyrroline N-oxide (DMPO), while singlet oxygen signals were captured using 2, 2, 6, 6-tetramethylpiperidine (TEMP). Electron spin resonance (ESR) spectra were meticulously recorded in dark conditions. Then above CDs solution was irradiated with instrument-equipped xenon lamp (5000 W/m²) for 10 min and collected signal again.

Culture of *B. Cinerea*, *Phytophthora* and *P. Capsici*

Botrytis cinerea and *S. sclerotiorum* were cultivated on potato dextrose agar (PDA, Solarbio, Beijing, China) plates at 25 °C in darkness until the mycelia completely colonized the plates. The *P. capsici* was grown on 10% (vol/vol) V8 medium plate at 25 °C in the dark.

Plant growth conditions

Tomato and *N. benthamiana* seeds were germinated under 28 °C for 5 days and then sown into the coco and peat mixture soil. Mature plants were cultured in the incubator with a 12 h photoperiod at the temperature of 25–28 °C.

Immunostimulatory treatment of plants

According to the results of preliminary experiments, 240 mg/L CDs was used for immune stimulation. CDs solution (2 mL per plant) was sprayed on the two-month-old tomato leaves and one-month-old *N. benthamiana* leaves. The control group were sprayed with the same volume of deionized water. Then the spray treated plants were used for RNA-seq, enzyme activity evaluation and ROS burst characterization and in planta infection.

In planta infection of *B. Cinerea*

The agar pieces with growing hyphae (diameter of 0.6 cm) were dipped in CDs solution (480 mg/L) or deionized water (control), following with sunlight irradiation (simulated with Xenon lamp with light intensity of 9.4×10^4 lux) for 30 min. Subsequently, these treated hyphae were inoculated to tomato leaves (1-month-old). After treatment for 5 days, the number of diseased leaves was recorded, and the lesion area of leaf was measured by Image J software (The National Institutes of health (NIH), Washington, DC, USA).

Quantification and statistical analysis

All boxplots and bar plots were generated by GraphPad Prism 10 (National institutes of health, San Diego, CA, USA). Statistical significance was determined by one-way ANOVA or Student's *t*-test.

Acknowledgements

We acknowledge the support from Natural Science Foundation of China (22377076 and 22074046), Natural Science Foundation of Guangdong Province (2022A1515010887), Shanghai Pujiang Program (to Huan Z., 22PJ1408500). E. K. thanks the China Postdoctoral Science Foundation (2023M732270) and the Postdoctoral Fellowship Program of CPSF (GZB20230425). We acknowledge support of a Burroughs Wellcome Fund Career Award at the Scientific Interface (CASI) (MPL), a Dreyfus foundation teacher-scholar award (MPL), the Philomathia foundation (MPL), an NSF CAREER award 2046159 (MPL), a Moore Foundation Award (MPL) and a polymath's award from Schmidt Sciences, LLC (MPL). MPL is a Chan Zuckerberg Biohub investigator and a Hellen Wills Neuroscience Institute Investigator.

Conflict of interest

The authors declare that they have no competing interests.

Author contributions

Huan Zhang and E.K. conceived the idea and designed the study. E.K. performed the experiments and data analysis and wrote the manuscript. M.L. and Honglu Zhang offer valuable suggestions to enhance the project, Huan Zhang, Honglu Zhang and M.L. revised the manuscript. X.C., Z.L., J.Y. and D.L. participated in data collection.

Data availability statement

The data that supports the findings of this study are available in the supplementary material of this article.

References

- Agrawal, G.K., Rakwal, R., Tamogami, S., Yonekura, M., Kubo, A. and Saji, H. (2002) Chitosan activates defense/stress response (s) in the leaves of *Oryza sativa* seedlings. *Plant Physiol. Biochem.* **40**, 1061–1069.
- Apel, K. and Hirt, H. (2004) Reactive oxygen species: metabolism, oxidative stress, and signal transduction. *Annu. Rev. Plant Biol.* **55**, 373–399.
- Bacete, L., Mérida, H., Miedes, E. and Molina, A. (2017) Plant cell wall-mediated immunity: cell wall changes trigger disease resistance responses. *Plant J.* **93**, 614–636.
- Bethke, G., Unthan, T., Uhrig, J.F., Pöschl, Y., Gust, A.A., Scheel, D. and Lee, J. (2009) Flg22 regulates the release of an ethylene response factor substrate from MAP kinase 6 in *Arabidopsis thaliana* via ethylene signaling. *Proc. Natl Acad. Sci. USA*, **106**, 8067–8072.
- Chandra, S., Pradhan, S., Mitra, S., Patra, P., Bhattacharya, A., Pramanik, P. and Goswami, A. (2014) High throughput electron transfer from carbon dots to chloroplast: a rationale of enhanced photosynthesis. *Nanoscale*, **6**, 3647–3655.
- Chen, X.-L., Wang, Z. and Liu, C. (2016) Roles of peroxisomes in the rice blast fungus. *Biomed. Res. Int.* **2016**, 9343417.
- Chen, R., Ma, D., Bao, Y., Wang, W., Du, D., Chen, X., Dou, D. et al. (2024) Joint application of plant immunity-inducing elicitors and fungicides to control *Phytophthora* diseases. *Phytopathol. Res.* **6**, 14.
- Cheng, Q., Zhang, T., Wang, Q., Wu, X., Li, L., Lin, R., Zhou, Y. et al. (2024) Photocatalytic carbon dots-triggered pyroptosis for whole cancer cell vaccines. *Adv. Mater.* **36**, 2408685.
- Cheung, N., Tian, L., Liu, X. and Li, X. (2020) The destructive fungal pathogen *Botrytis cinerea*—insights from genes studied with mutant analysis. *Pathogens*, **9**, 923.
- Denness, L., McKenna, J.F., Segonzac, C., Wormit, A., Madhou, P., Bennett, M., Mansfield, J. et al. (2011) Cell wall damage-induced lignin biosynthesis is regulated by a reactive oxygen species- and jasmonic acid-dependent process in *Arabidopsis*. *Plant Physiol.* **156**, 1364–1374.
- Dewen, Q., Yijie, D., Yi, Z., Shupeng, L. and Fachao, S. (2017) Plant immunity inducer development and application. *Mol. Plant-Microbe Interact.* **30**, 355–360.
- Domergue, F., Vishwanath, S.J., Joubès, J., Ono, J. and Rowland, O. (2010) Three *Arabidopsis* fatty acyl-coenzyme A reductases, FAR1, FAR4, and FAR5, generate primary fatty alcohols associated with suberin deposition. *Plant Physiol.* **153**, 1539.
- El-Baky, N.A. and Amara, A.A.A.F. (2021) Recent approaches towards control of fungal diseases in plants: An updated review. *J. Fungi*, **7**, 900.
- El-Shetehy, M., Moradi, A., Maceroni, M., Reinhardt, D., Petri-Fink, A., Rothen-Rutishauser, B., Mauch, F. et al. (2021) Silica nanoparticles enhance disease resistance in *Arabidopsis* plants. *Nat. Nanotechnol.* **16**, 344–353.
- Ge, D., Yeo, I.-C. and Shan, L. (2022) Knowing me, knowing you: self and non-self recognition in plant immunity. *Essays Biochem.* **66**, 447–458.
- Görlach, J., Volrath, S., Knauf-Beiter, G., Hengy, G., Beckhove, U., Kogel, K.-H., Oostendorp, M. et al. (1996) Benzothiadiazole, a novel class of inducers of systemic acquired resistance, activates gene expression and disease resistance in wheat. *Plant Cell*, **8**, 629–643.
- Guirguis, A., Yang, W., Conlan, X.A., Kong, L., Cahill, D.M. and Wang, Y. (2023) Boosting plant photosynthesis with carbon dots: a critical review of performance and prospects. *Small*, **19**, e2300671.
- Guo, Z., Chen, Q., Liang, T., Zhou, B., Huang, S., Cao, X., Wang, X. et al. (2023) Functionalized carbon nano-enabled plant ROS signal engineering for growth/defense balance. *Nano Today*, **53**, 102045.
- Hegde, M.L., Hazra, T.K. and Mitra, S. (2008) Early steps in the DNA base excision/single-strand interruption repair pathway in mammalian cells. *Cell Res.* **18**, 27–47.
- Hou, S., Liu, D. and He, P. (2021) Phytocytokines function as immunological modulators of plant immunity. *Stress Biol.* **1**, 8.
- Hu, L., Sun, Y., Zhou, Y., Bai, L., Zhang, Y., Han, M., Huang, H. et al. (2017) Nitrogen and sulfur co-doped chiral carbon quantum dots with independent photoluminescence and chirality. *Inorg. Chem. Front.* **4**, 946–953.
- Hu, H., Cheng, W., Wang, X., Yang, Y., Yu, X., Ding, J., Lin, Y. et al. (2024) Enhancing plant photosynthesis using carbon dots as light converter and

- photosensitizer. *bioRxiv*, 2024.02.06.579025. <https://doi.org/10.1101/2024.02.06.579025>
- Huang, X., Lin, J., Liang, J., Kou, E., Cai, W., Zheng, Y., Zhang, H. *et al.* (2023) Pyridinic nitrogen doped carbon dots supply electrons to improve photosynthesis and extracellular electron transfer of *Chlorella pyrenoidosa*. *Small*, **19**, 2206222.
- Jelenska, J., Davern, S.M., Standaert, R.F., Mirzadeh, S. and Greenberg, J.T. (2017) Flagellin peptide flg22 gains access to long-distance trafficking in *Arabidopsis* via its receptor, FLS2. *J. Exp. Bot.* **68**, 1769–1783.
- Jeon, S.J., Zhang, Y., Castillo, C., Nava, V., Ristroph, K., Therrien, B., Meza, L. *et al.* (2023) Targeted delivery of sucrose-coated nanocarriers with chemical cargoes to the plant vasculature enhances long-distance translocation. *Small*, **20**, e2304588.
- Jing, H., Wenyi, J., Xuefeng, Y., Chuanhao, Y., White, J.C., Junfeng, L., Guofeng, S. *et al.* (2022) Carbon dots improve the nutritional quality of coriander (*Coriandrum sativum* L.) by promoting photosynthesis and nutrient uptake. *Environ. Sci. Nano*, **5**, 9.
- Jo, Y.-K., Kim, B.H. and Jung, G. (2009) Antifungal activity of silver ions and nanoparticles on phytopathogenic fungi. *Plant Dis.* **93**, 1037–1043.
- Karimi, E. (2019) Antimicrobial activities of nanoparticles. In *Nanotechnology for Agriculture: Crop Production & Protection* (Panpatte, D.G. and Jhala, Y.K., eds), pp. 171–206. Singapore: Springer.
- Khosropour, E., Hakimi, L. and Weisany, W. (2023) Chapter 12 – Role of engineered nanomaterials in biotic stress managements. In *Engineered Nanomaterials for Sustainable Agricultural Production, Soil Improvement and Stress Management* (Husen, A., ed), pp. 257–272. Cambridge, MA: Academic Press.
- Kou, E., Yao, Y., Yang, X., Song, S., Li, W., Kang, Y., Qu, S. *et al.* (2021) Regulation mechanisms of carbon dots in the development of lettuce and tomato. *ACS Sustain. Chem. Eng.* **9**, 944–953.
- Kou, E., Li, W., Lin, J., Zhang, H., Zhang, X., Liu, Y. and Lei, B. (2023) Self-assembled photosensitive carbon nanocrystals with broad-spectrum antibacterial bioactivity. *J. Mater. Chem. A*, **11**, 3060–3069.
- Lamour, K.H., Stam, R., Jupe, J. and Huitema, E. (2011) The oomycete broad-host-range pathogen *Phytophthora capsici*. *Mol. Plant Pathol.* **13**, 329–337.
- Li, H., Huang, J., Liu, Y., Lu, F., Zhong, J., Wang, Y., Li, S. *et al.* (2019) Enhanced RuBisCO activity and promoted dicotyledons growth with degradable carbon dots. *Nano Res.* **12**, 1585–1593.
- Li, Y., Pan, X., Xu, X., Wu, Y., Zhuang, J., Zhang, X., Zhang, H. *et al.* (2021) Carbon dots as light converter for plant photosynthesis: augmenting light coverage and quantum yield effect. *J. Hazard. Mater.* **410**, 124534.
- Li, Y., Tang, Z., Pan, Z., Wang, R., Wang, X., Zhao, P., Liu, M. *et al.* (2022) Calcium-mobilizing properties of *Salvia miltiorrhiza*-derived carbon dots confer enhanced environmental adaptability in plants. *ACS Nano*, **16**, 4357–4370.
- Lin, L., Zhang, X., Fan, J., Li, J., Ren, S., Gu, X., Li, P. *et al.* (2024) Natural variation in BnaA07.MKK9 confers resistance to Sclerotinia stem rot in oilseed rape. *Nat. Commun.* **15**, 5059.
- Liu, J., Li, R. and Yang, B. (2020) Carbon dots: a new type of carbon-based nanomaterial with wide applications. *ACS Cent. Sci.* **6**, 2179–2195.
- Liu, Y.-Y., Yu, N.-Y., Fang, W.-D., Tan, Q.-G., Ji, R., Yang, L.-Y., Wei, S. *et al.* (2021) Photodegradation of carbon dots cause cytotoxicity. *Nat. Commun.* **12**, 812.
- Liu, Y., Liu, D., Han, X., Chen, Z., Li, M., Jiang, L. and Zeng, J. (2024) Magnesium-doped carbon quantum dot nanomaterials alleviate salt stress in rice by scavenging reactive oxygen species to increase photosynthesis. *ACS Nano*, **18**, 31188–31203.
- Lu, S., Sui, L., Liu, J., Zhu, S., Chen, A., Jin, M. and Yang, B. (2017) Near-infrared photoluminescent polymer–carbon nanodots with two-photon fluorescence. *Adv. Mater.* **29**, 1603443.
- Mittler, R. (2017) ROS are good. *Trends Plant Sci.* **22**, 11–19.
- Mittler, R., Vanderauwera, S., Gollery, M. and Van Breusegem, F. (2004) Reactive oxygen gene network of plants. *Trends Plant Sci.* **9**, 490–498.
- Molina, A., Jordá, L., Torres, M.Á., Martín-Dacal, M., Berlanga, D.J., Fernández-Calvo, P., Gómez-Rubio, E. *et al.* (2024) Plant cell wall-mediated disease resistance: current understanding and future perspectives. *Mol. Plant*, **17**, 699–724.
- Murchie, E.H. and Lawson, T. (2013) Chlorophyll fluorescence analysis: a guide to good practice and understanding some new applications. *J. Exp. Bot.* **64**, 3983–3998.
- Nelson, R., Wiesner-Hanks, T., Wissner, R. and Balint-Kurti, P. (2018) Navigating complexity to breed disease-resistant crops. *Nat. Rev. Genet.* **19**, 21–33.
- Nie, H., Li, M., Li, Q., Liang, S., Tan, Y., Sheng, L., Shi, W. *et al.* (2014) Carbon dots with continuously tunable full-color emission and their application in ratiometric pH sensing. *Chem. Mater.* **26**, 3104–3112.
- Nosaka, Y. and Nosaka, A.Y. (2017) Generation and detection of reactive oxygen species in photocatalysis. *Chem. Rev.* **117**, 11302–11336.
- Nürnberg, T. and Scheel, D. (2001) Signal transmission in the plant immune response. *Trends Plant Sci.* **6**, 372–379.
- Qi, J., Wang, J., Gong, Z. and Zhou, J.M. (2017) Apoplastic ROS signaling in plant immunity. *Curr. Opin. Plant Biol.* **38**, 92–100.
- Raffaale, S., Leger, A. and Roby, D. (2009) Very long chain fatty acid and lipid signaling in the response of plants to pathogens. *Plant Signal. Behav.* **4**, 94–99.
- Romanazzi, G. and Feliziani, E. (2014) *Botrytis cinerea* (Gray Mold). In *Postharvest Decay* (Bautista-Baños, S., ed), pp. 131–146. San Diego, CA: Academic Press.
- Ru, Y., Sui, L., Song, H., Liu, X., Tang, Z., Zang, S.-Q., Yang, B. *et al.* (2021) Rational design of multicolor-emitting chiral carbonized polymer dots for full-color and white circularly polarized luminescence. *Angew. Chem. Int. Ed. Engl.* **133**, 14210–14218.
- Ru, Y., Zhang, B., Yong, X., Sui, L., Yu, J., Song, H. and Lu, S. (2023) Full-color circularly polarized luminescence of CsPbX₃ nanocrystals triggered by chiral carbon dots. *Adv. Mater.* **35**, 2207265.
- Santana, I., Jeon, S.-J., Kim, H.-I., Islam, M.R., Castillo, C., Garcia, G.F.H., Newkirk, G.M. *et al.* (2022) Targeted carbon nanostructures for chemical and gene delivery to plant chloroplasts. *ACS Nano*, **16**, 12156–12173.
- Seifert, G.J. and Blaukopf, C. (2010) Irritable walls: the plant extracellular matrix and signaling. *Plant Physiol.* **153**, 467–478.
- Shang, H., Ma, C., Li, C., Cai, Z., Shen, Y., Han, L., Wang, C. *et al.* (2023) Aloe vera extract gel-biosynthesized selenium nanoparticles enhance disease resistance in lettuce by modulating the metabolite profile and bacterial endophytes composition. *ACS Nano*, **17**, 13672–13684.
- Sharma, S., Perring, T.M., Jeon, S.-J., Huang, H., Xu, W., Islamovic, E., Sharma, B. *et al.* (2024) Nanocarrier mediated delivery of insecticides into tarsi enhances stink bug mortality. *Nat. Commun.* **15**, 9737.
- Singh, R. and Chandrawat, K.S. (2017) Role of phytoalexins in plant disease resistance. *Int. J. Curr. Microbiol. App. Sci.* **6**, 125–129.
- Sukhanova, R.A. (2010) Fluorescent quantum dots as artificial antennas for enhanced light harvesting and energy transfer to photosynthetic reaction centers. *Angew. Chem.* **49**(40), 7217–7221.
- Swaminathan, S., Lionetti, V. and Zabolina, O.A. (2022) Plant cell wall integrity perturbations and priming for defense. *Plan. Theory*, **11**, 3539.
- Vanholme, R., Demedts, B., Morreel, K., Ralph, J. and Boerjan, W. (2010) Lignin biosynthesis and structure. *Plant Physiol.* **153**, 895–905.
- Wang, G.F. and Balint-Kurti, P. (2016) Maize homologs of CCoAOMT and HCT, two key enzymes in lignin biosynthesis, form complexes with the NLR Rp1 protein to modulate the defense response. *Plant Physiol.* **171**, 2166–2177.
- Wang, W., Li, G., Xia, D., An, T., Zhao, H. and Wong, P.K. (2017) Photocatalytic nanomaterials for solar-driven bacterial inactivation: recent progress and challenges. *Environ. Sci. Nano*, **4**, 782–799.
- Wang, C., Yang, H., Chen, F., Yue, L., Wang, Z. and Xing, B. (2021) Nitrogen-doped carbon dots increased light conversion and electron supply to improve the corn photosystem and yield. *Environ. Sci. Technol.* **55**, 12317–12325.
- Wang, C., Ji, Y., Cao, X., Yue, L., Chen, F., Li, J., Yang, H. *et al.* (2022) Carbon dots improve nitrogen bioavailability to promote the growth and nutritional quality of soybeans under drought stress. *ACS Nano*, **16**, 12415–12424.
- de Weck, A.L. (1983) Penicillins and Cephalosporins. In *Allergic Reactions to Drugs* (de Weck, A.L. and Bundgaard, H., eds), pp. 423–482. Berlin, Heidelberg: Springer Berlin Heidelberg.
- Wei, L., Wu, H., Zhang, X., Zhang, J. and Zhuang, S. (2017) Enhanced biological photosynthetic efficiency using light-harvesting engineering with dual-emissive carbon dots. *Adv. Funct. Mater.* **28**, 1804004.

- Williams, J.S., Hall, S.A., Hawkesford, M.J., Beale, M.H. and Cooper, R.M. (2002) Elemental sulfur and thiol accumulation in tomato and defense against a fungal vascular pathogen. *Plant Physiol.* **128**, 150–159.
- Wu, C., Wang, C., Han, T., Zhou, X., Guo, S. and Zhang, J. (2013) Insight into the cellular internalization and cytotoxicity of graphene quantum dots. *Adv. Healthc. Mater.* **2**, 1613–1619.
- Wu, B., Qi, F. and Liang, Y. (2023) Fuels for ROS signaling in plant immunity. *Trends Plant Sci.* **28**, 1124–1131.
- Xia, X., Shi, B., Wang, L., Liu, Y., Zou, Y., Zhou, Y., Chen, Y. et al. (2021) From mouse to mouse-ear cress: nanomaterials as vehicles in plant biotechnology. *Exploration (Beijing, China)*, **1**, 9–20.
- Yang, B., Yang, S., Zheng, W. and Wang, Y. (2022) Plant immunity inducers: from discovery to agricultural application. *Stress Biol.* **2**, 5.
- Yang, H., Wang, C., Chen, F., Yue, L., Cao, X., Li, J., Zhao, X. et al. (2022) Foliar carbon dot amendment modulates carbohydrate metabolism, rhizospheric properties and drought tolerance in maize seedling. *Sci. Total Environ.* **809**, 151105.
- Yoshioka, H., Bouteau, F. and Kawano, T. (2008) Discovery of oxidative burst in the field of plant immunity: looking back at the early pioneering works and towards the future development. *Plant Signal. Behav.* **3**, 153–155.
- Yoshioka, H., Hino, Y., Iwata, K., Ogawa, T., Yoshioka, M., Ishihama, N. and Adachi, H. (2023) Dynamics of plant immune MAPK activity and ROS signaling in response to invaders. *Physiol. Mol. Plant Pathol.* **125**, 102000.
- Yu, C., Zhang, B., Yan, F., Zhao, J., Li, J., Li, L. and Li, J. (2016) Engineering nano-porous graphene oxide by hydroxyl radicals. *Carbon*, **105**, 291–296.
- Yuan, M., Jiang, Z., Bi, G., Nomura, K., Liu, M., Wang, Y., Cai, B. et al. (2021) Pattern-recognition receptors are required for NLR-mediated plant immunity. *Nature*, **592**, 105–109.
- Yue, J., Zhang, K., Yu, H., Yu, L., Hou, T., Chen, X., Ge, H. et al. (2019) Mechanism insights into tunable photoluminescence of carbon dots by hydroxyl radicals. *J. Mater. Sci.* **54**, 6140–6150.
- Zhang, M. and Zhang, S. (2022) Mitogen-activated protein kinase cascades in plant signaling. *J. Integr. Plant Biol.* **64**, 301–341.
- Zhang, H., Wang, G., Zhang, Z., Lei, J.H., Liu, T.-M., Xing, G., Deng, C.-X. et al. (2022) One step synthesis of efficient red emissive carbon dots and their bovine serum albumin composites with enhanced multi-photon fluorescence for in vivo bioimaging. *Light Sci. Appl.* **11**, 113.
- Zhang, Y., Jia, Q., Nan, F., Wang, J., Liang, K., Li, J., Xue, X. et al. (2023) Carbon dots nanophotosensitizers with tunable reactive oxygen species generation for mitochondrion-targeted type VII photodynamic therapy. *Biomaterials*, **293**, 121953.
- Zhu, F., Cao, M.-Y., Zhang, Q.-P., Mohan, R., Schar, J., Mitchell, M., Chen, H. et al. (2024) Join the green team: inducers of plant immunity in the plant disease sustainable control toolbox. *J. Adv. Res.* **57**, 15–42.

Supporting information

Additional supporting information may be found online in the Supporting Information section at the end of the article.

Methods S1 Degradability of CDs.

Methods S2 Detection of ROS burst.

Methods S3 Location of CDs In Plants of *N. benthamiana*.

Methods S4 *In vivo* Inoculation of *B. cinerea* and *P. capsici*.

Methods S5 Evaluation of enzyme activity.

Methods S6 RNA extraction and RNA- Sequencing (RNA- Seq) of tomato leaves.

Methods S7 Determination of chlorophyll fluorescence.

Methods S8 Evaluation of CDs impact on plant growth.

Methods S9 Effects of CDs concentrations on *B. cinerea* mycelium growth.

Methods S10 RNA-seq of *B. cinerea*.

Methods S11 SEM and TEM characterization.

Table S1 Primers sequence for qRT-PCR.

Figure S1 Zeta potential of CDs aqueous solution.

Figure S2 Characterization of CDs under nature sunlight.

Figure S3 CDs distribution in *N. benthamiana* leaf after CDs spray treatment (480 mg/L, 2 mL) for 4 h.

Figure S4 ROS signal in *N. benthamiana* leaves after spray with Flg22 solution (250 µg/L, 2 mL per plant) for 6 hours.

Figure S5 ROS burst detected with the fluorescent dye H₂DCFDA in tomato leaf after spray treatment with CDs (240 mg/L) or deionized water for 6 h (2 mL for each plant).

Figure S6 Disease leaves and incidence ratio of tomato (a) and *N. benthamiana* (b) after in planta infection with *B. cinerea* hyphae for 5 days.

Figure S7 Disease leaves of tomato and incidence ratio after in planta infection with *P. capsici* spores (20 µL per leaf, 1 × 10⁵ zoospores per mL) for 7 days.

Figure S8 CDs induced (240 mg/L) immunity response on transcriptional level.

Figure S9 Relative expression level of partial DEGs in the first ten KEGG pathways.

Figure S10 Impact of CDs spray treatment on photosynthetic performance of *N. benthamiana* leaves. Quantum yield of PSI (a), PSII (b) and maximum quantum efficiency (c) of PSII photochemistry (Fv/Fm) 72 hours after sprayed by various concentration of CDs.

Figure S11 Above ground fresh weight (a) and dry weight (b) of *N. benthamiana* measured at 7 days after spray treatment with 240 or 480 mg/L CDs or deionized water (0 mg/L), 2 mL per plant.

Figure S12 Tomato fruit yields after spray treatment with 240 or 480 mg/L CDs or deionized water (0 mg/L) for 30 days, 2 mL per plant. Data show means ± s.e.m.

Figure S13 (a) Images of *B. cinerea* hyphae after treated by Light + CDs (with concentrations of 160, 240, 480 and 960 mg/L) for 30 minutes. Scale bar = 4 cm. (b) Statistical data of growth inhibition ratio of *B. cinerea* hyphae. (c) Representative images of spore's germination of *B. cinerea* under different treatment.

Figure S14 Tomato leaves of control group (infected by light treated hyphae) and the CDs group (infected by Light + CDs treated hyphae, where the concentration of CDs is 480 mg/L and the volume is 1 mL). Diseased leaves were marked with red triangles in the picture.